Neuron, Vol. 23, 607–615, July, 1999, Copyright ©1999 by Cell Press

Mechanisms Underlying Phasic and Sustained Secretion in Chromaffin Cells from Mouse Adrenal Slices

Thomas Voets,* Erwin Neher, and Tobias Moser
Department of Membrane Biophysics
Max-Planck-Institute for Biophysical Chemistry
Am Fassberg 11
D-37077 Göttingen
Federal Republic of Germany

Summary

Many neurosecretory preparations display two components of depolarization-induced exocytosis: a phasic component synchronized with Ca^{2+} channel opening, followed by a slower sustained component. We evaluated possible mechanisms underlying this biphasic behavior by stimulating mouse chromaffin cells in situ with both depolarizations and flash photolysis of caged Ca^{2+}. From a direct comparison of the secretory responses to both stimuli, we conclude that phasic and sustained release components originate from a readily releasable pool (RRP) of equally fusion-competent vesicles, suggesting that differences in the vesicles' proximity to Ca^{2+} channels underlie the biphasic secretory behavior. An intermediate pool in dynamic equilibrium with the RRP ensures rapid recruitment of release-ready vesicles after RRP depletion. Our results are discussed in terms of a refined model for secretion in chromaffin cells.

Introduction

It is generally known that the opening of Ca^{2+} channels elicits an intracellular Ca^{2+} signal with a highly nonuniform spatial distribution (for a recent review, see Neher, 1998). Theoretical calculations indicate that within a microdomain of 10–20 nm around an open channel, peak Ca^{2+} concentrations can be >10-fold higher than at 100–200 nm from the sites of Ca^{2+} entry. These steep Ca^{2+} gradients have a profound influence on the kinetics of depolarization-induced neurosecretion. Due to the third- or fourth-power relation between secretory rate and $[Ca^{2+}]_i$ (Dodge and Rahamimoff, 1967; Heidelberger et al., 1994; Heinemann et al., 1994), vesicles proximal to Ca^{2+} channels are expected to be released several orders of magnitude faster than equally fusion-competent but more distal vesicles.

Depolarization-induced secretion in neurosecretory cells often displays two kinetic components: a fast phasic component, highly synchronous with the opening of Ca^{2+} channels, followed by a slower and more sustained component (Rahamimoff and Yaari, 1973; Goda and Stevens, 1994; Horrigan and Bookman, 1994; Hsu and Jackson, 1996; Mennerick and Matthews, 1996; Moser and Neher, 1997b; Sakaba et al., 1997; von Gersdorff et al., 1998; Yawo, 1999). The exact mechanisms underlying this biphasic secretory behavior remains a matter of debate. Given the spatial inhomogeneity of the Ca^{2+} signal discussed above, these two components might originate from a homogenous population of equally fusion-competent vesicles that differ in their proximity to Ca^{2+} channels. However, the existence of two biochemically and/or morphologically distinct vesicle pools exhibiting intrinsically different fusion rates can equally well account for the observation of both phasic and sustained release components. For example, different isoforms of the putative Ca^{2+} sensor synaptotagmin have been suggested to underlie both forms of release (Geppert et al., 1994).

In the present study, we addressed this question in mouse adrenal chromaffin cells in situ, by directly comparing secretory responses to depolarizations with those to spatially uniform increases in $[Ca^{2+}]_i$ after flash photolysis of the photolabile Ca^{2+} chelator nitrophenyl-EGTA (NP-EGTA). Exocytosis was monitored by means of patch-clamp measurements of cell membrane capacitance (Neher and Marty, 1982), while $[Ca^{2+}]_i$ was simultaneously estimated using the calcium indicators Fura-2 or Furaptra (Grynkiewicz et al., 1985). The sizes of the vesicle pools that underlie the fast and slow secretory responses were quantified using paired depolarizations (Gillis et al., 1996) and compared with flash responses in the same cells. We find that a readily releasable pool (RRP) of ~140 equally fusion-competent vesicles underlies both the fast phasic and the slower sustained secretory responses to depolarizations. About 25% of the vesicles in the RRP appear to be located in the close vicinity of Ca^{2+} channels, such that they can be rapidly released in response to brief depolarizations. Fusion of the remaining 75% of the readily releasable vesicles occurs only after longer or repeated depolarizations, indicating that these vesicles are more distal to Ca^{2+} channels. In addition, responses to flash photolysis reveal an intermediate vesicle pool that is in dynamic equilibrium with the RRP and ensures a rapid resupply of release-ready vesicles after RRP depletion. Our results are explained in terms of a refined model for the secretion of chromaffin vesicles, in which both sequential and parallel processes precede the final fusion step.

Results

Two Phases of Exocytosis in Response to Trains of Depolarizations

Figure 1 illustrates the biphasic C_m increase in response to increasing amounts of voltage-dependent Ca^{2+} influx in mouse chromaffin cells in situ. A representative example of the C_m increase evoked by a train of 10 ms depolarizations to 0 mV at 18 Hz is shown in Figure 1A. This cell reached a first plateau ΔC_m level of about 60 fF between the fifth and the eighth depolarization before onset of a second larger bout of exocytosis. At a lower stimulation frequency of 3 Hz, this second, slower phase of exocytosis was not evoked unless the duration of the

*To whom correspondence should be addressed (e-mail: tvoets@gwdg.de).

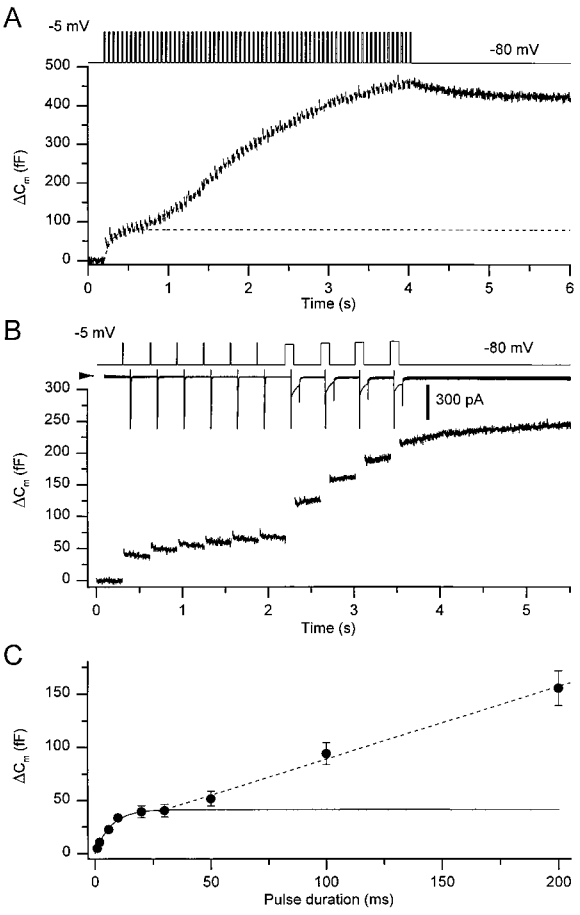

Figure 1. Two Components of Depolarization-Induced Exocytosis

(A) Example of the capacitance response (ΔC_m) to a train of 10 ms depolarizations delivered at 18 Hz (top). The dotted line is an exponential function drawn to indicate the first plateau C_m level.

(B) Average current and ΔC_m from 10 cells in response to a stimulation protocol consisting of six 10 ms depolarizations followed by four 100 ms depolarizations delivered 300 ms apart. The potentials for the 100 ms depolarizations were chosen to compensate for Ca^{2+} current inactivation and thus ensure comparable Ca^{2+} influx.

(C) Plot showing the relation between pulse duration (depolarization to −5 mV) and ΔC_m. C_m was analyzed in a time window between 1 and 2.5 s after the depolarization. The solid line represents a monoexponential fit for pulses between 1 and 30 ms. The dotted line is a linear fit for pulses between 30 and 200 ms. Each data point represents pooled data from at least 15 cells.

depolarizations was increased (Figure 1B). After longer depolarizations, we often observed a slow increase in C_m that persisted for some time after Ca^{2+} entry had stopped (Figure 1B), a phenomenon that has been previously attributed to diffusion of Ca^{2+} between Ca^{2+} channels and release sites (Chow et al., 1994). Figure 1C shows the relationship between the duration of depolarizations and the evoked C_m increase. The capacitance response reaches a plateau for pulses between 20 and 50 ms. A single exponential fit to the response to depolarizations between 1 and 30 ms yielded a rate constant of 150 s^{-1} and an amplitude of 45 fF, which corresponds to ~35 vesicles using the conversion factor of 1.3 fF per vesicle (Moser and Neher, 1997a). These results confirm the existence of a small RRP (Moser and Neher, 1997b) and shows that this pool can be selectively and rapidly depleted by mild stimulation. We adopted the term immediately releasable pool (IRP) for this vesicle population, as proposed in a recent study on rat chromaffin cells (Horrigan and Bookman, 1994). After depletion of the IRP, exocytosis initially proceeds at a maximal rate of 520 vesicles/s. The progressive decline of the C_m responses to the repeated 100 ms depolarizations (Figure 1B) suggests the existence of a larger but limited RRP (Heinemann et al., 1993; Horrigan and Bookman, 1994). However, as recovery of the RRP in chromaffin cells (Moser and Neher, 1997b; Smith et al., 1998) occurs with a time constant of ~10 s, the stimulation protocols presented in Figures 1A–1B may be too long to yield reliable pool size estimates.

In order to quantitate the pool sizes more rigorously, we made use of dual-pulse protocols (Gillis et al., 1996). From the sum and the ratio of the capacitance increases to two qualitatively equivalent Ca^{2+} current injections applied at a short interval, the upper limit of a releasable pool can be derived according to:

$$B_{max} = \frac{S}{1 - R^2} \quad (1)$$

where S represents the sum of the capacitance responses to the first (ΔC_{m1}) and the second (ΔC_{m2}) depolarizations, and R is the ratio $\Delta C_{m2}/\Delta C_{m1}$. S itself can be used as a lower pool size estimate, assuming that recovery during the 300 ms interpulse intervals can be neglected. The potentials of the two depolarizing stimuli were adjusted to give equal amounts of Ca^{2+} influx. Provided that the second stimulus is at least as strong as the first, values for R of <1 represent secretory depression, presumably due to partial pool depletion. For analyses, only cells with R of <0.7 were used, as substantial pool depletion is a prerequisite for accurate pool size determinations. This requirement was met by the large majority (>90%) of the cells (see Gillis et al., 1996, for a detailed description of the dual-pulse paradigm and its limitations).

We used two different dual-pulse protocols: the dual 10 ms protocol served for the estimation of the size of IRP, whereas the dual 100 ms protocol was used to quantitate the whole RRP, including the IRP. Figure 2A shows, at low time resolution, an experiment where we simultaneously measured $[Ca^{2+}]_i$ and C_m. The gaps in both $[Ca^{2+}]_i$ and C_m traces represent episodes during which C_m was measured at high time resolution and the dual 100 ms (first and third gap) and dual 10 ms (second and fourth gap) protocols were applied. Note that the dual 100 ms protocol induces a rise in global $[Ca^{2+}]_i$ to >1 μM, whereas the dual 10 ms protocol causes hardly any change in $[Ca^{2+}]_i$. Figure 2B shows the C_m response to the first dual 10 ms protocol at high time resolution. Whereas the current response to both depolarizations was fairly constant (inset), the C_m jump after the second depolarization was clearly depressed (R = 0.42), indicative of depletion of the IRP. A similar degree of secretory depression (R = 0.38) was observed for the dual 100 ms protocol (Figure 2C). From 21 analogous experiments, we estimated the RRP size to lie between 120 and 150 vesicles, of which 30–40 vesicles belong to the

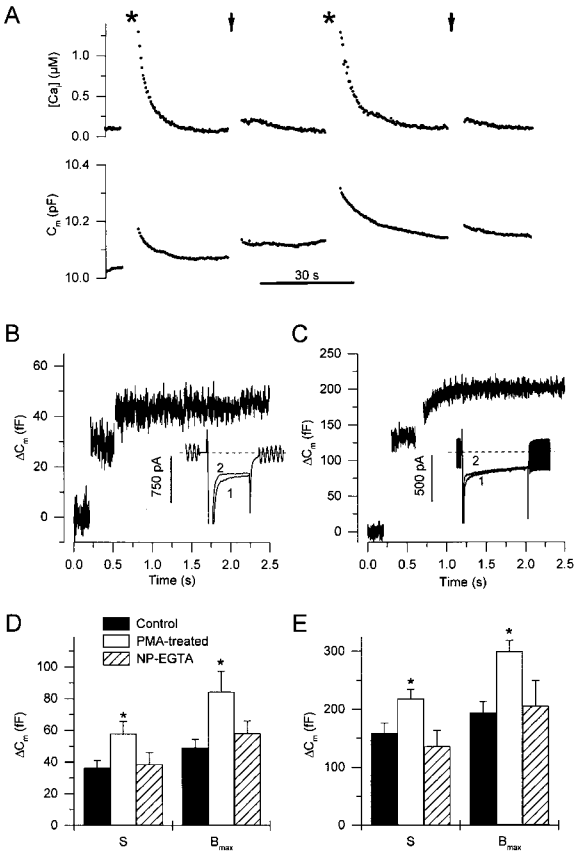

Figure 2. Pool Size Estimates Using Dual-Pulse Protocols

(A) Simultaneous measurement of $[Ca^{2+}]_i$ (using Fura-2) and membrane capacitance at low time resolution. The gaps in both traces indicate the periods during which the dual 10 ms (arrowheads) or dual 100 ms (asterisks) protocols were applied and C_m was measured at high time resolution. Note the occurrence of compensatory endocytosis following the stimuli. In 21 similar experiments, $[Ca^{2+}]_i$ increased from an average basal level of 101 ± 13 nM to 158 ± 26 nM and 954 ± 74 nM after the dual 10 ms and dual 100 ms protocols, respectively.

(B) High-resolution C_m recording of the response to the first dual 10 ms protocol. The whole-cell currents recorded during the two depolarizations are overlaid in the inset. For clarity, the rapidly activating and inactivating inward Na^{2+} current of >2 nA at the beginning of the pulse was truncated.

(C) The same as (B) but for the second dual 100 ms protocol. To exclude an influence of Ca^{2+} current inactivation, the potentials of the two depolarizations in the dual-pulse protocol were adjusted to give the same total amount of Ca^{2+} influx (see Gillis et al., 1996). In this example, the depolarizing potentials were −10 and −5 mV. Dual-pulse experiments in which integrated Ca^{2+} currents differed by more than 10% between the first and the second stimulus were discarded from analysis.

(D) Average values for S and B_{max}, calculated from responses to the dual 10 ms protocol, for whole-cell recordings using pipette solution 1 (0.1 mM Fura-2 as main Ca^{2+} chelator) in the absence (closed bars, n = 21) or presence (open bars, n = 15) of 100 nM PMA in the bath, and for the 5 mM NP-EGTA containing pipette solution 2 (hatched bars, n = 16). Asterisk indicates statistical significance ($p < 0.05$).

(E) The same as (D) but for responses to the dual 100 ms protocol. The sum response was analyzed in a time window between 1 and 2 s after the second depolarization, hence taking post-pulse secretion into account.

IRP. Pool size estimates obtained with a pipette solution containing 5 mM NP-EGTA (75% Ca saturated) as the main Ca^{2+} buffer were not significantly different from those obtained with 100 μM Fura-2 as the main chelator (Figures 2D and 2E). This finding may seem somewhat surprising, considering the high concentration of NP-EGTA, which before photolysis acts as a Ca^{2+} buffer. However, this buffering effect is limited both by the high degree of Ca^{2+} saturation and by the relatively slow binding kinetics of NP-EGTA (similar to EGTA).

Stimulation of protein kinase C (PKC) has been shown to increase the amount of release-ready vesicles in a number of neurosecretory preparations (Gillis et al., 1996; Stevens and Sullivan, 1998; Yawo, 1999), and in goldfish retinal bipolar cells it selectively enhances the slow secretory component (Minami et al., 1998). As a first test to see whether vesicles in the IRP are biochemically different from the rest of the RRP, we estimated the size of both pools after treating the cells with 100 nM phorbol 12-myristate 13-acetate (PMA), a potent PKC activator. We found an augmentation of both IRP and RRP to ~150% of their control values (Figures 2D and 2E), indicating that both pools are equally sensitive to phorbol ester stimulation.

Comparison of C_m Responses to Depolarizations and to Photorelease of Caged Ca^{2+}

To test the hypothesis that the IRP represents vesicles with a higher fusion competence than the remainder of the vesicles in the RRP, we set out to correlate C_m responses to depolarizations with C_m responses to spatially uniform $[Ca^{2+}]_i$ elevations after photorelease of NP-EGTA-bound calcium. Our basic assumption was that all vesicles with the same fusion competence would show up as single kinetic components in the C_m response to a rapid, spatially uniform elevation of $[Ca^{2+}]_i$. Figure 3A shows a representative C_m increase in response to a calcium jump to 25 μM. The time course of the C_m increase after a flash was always well fitted with the sum of three exponential terms, with, for this example, time constants of 27, 290, and 5600 ms, respectively. These kinetic properties are quantitatively very similar to previous results from isolated bovine chromaffin cells (Heinemann et al., 1994). The slowest kinetic component (time constant > 3 s) is most probably a mixture of exocytosis and endocytosis and was therefore not studied in more detail. The two faster kinetic components, which were generally over in ~1 s, have previously been termed the exocytic burst and were supposed to reflect fusion of release-ready vesicles that require only an elevation of $[Ca^{2+}]_i$ for exocytosis (Thomas et al., 1993; Xu et al., 1998).

To correlate the kinetic components of the exocytic burst with the C_m responses to voltage-dependent Ca^{2+} influx, we used protocols in which both types of stimuli, depolarizations and flash photolysis of caged Ca^{2+}, were triggered in rapid succession. This enabled us to investigate to what extent secretion induced by one type of stimulus affects the subsequent C_m response to the other type. As illustrated in Figure 3B, C_m responses to 100 ms depolarizations were completely suppressed for at least 4 s after a flash, indicating that a uniform rise in $[Ca^{2+}]_i$ to ~20 μM fully depletes the RRP. In contrast,

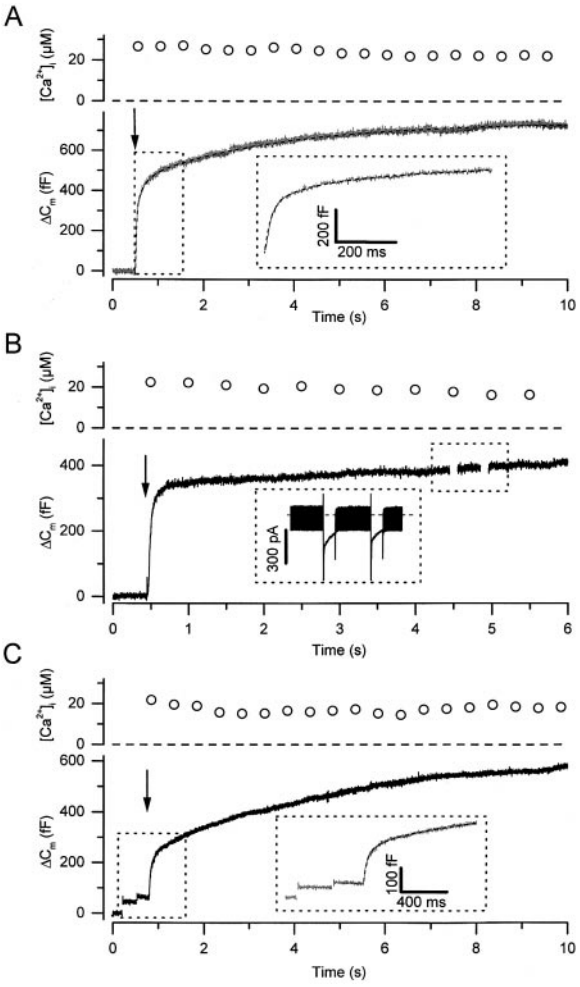

Figure 3. Capacitance Responses to a Combination of Depolarizations and Flash Photolysis of Caged Ca^{2+}

(A) Simultaneous recording of $[Ca^{2+}]_i$ (using Furaptra) and C_m in response to a flash. The flash response was well fitted by a triple exponential function with time constants of 27, 290, and 5600 ms, respectively (superimposed dashed line). The magnification of the boxed area shows the first second after the flash to illustrate the two kinetic components of the exocytic burst.

(B) Example of an experiment where the dual 100 ms protocol is applied 4 s after a flash. Ca^{2+} currents recorded after the flash were normal in amplitude (boxed area), indicating that the lack of response to the depolarizations is not due to Ca^{2+} current inactivation.

(C) Example of an experiment where a flash was applied 300 ms after the dual 10 ms protocol. The magnification of the boxed area shows that the two kinetic components of the exocytic burst are not eliminated by the preceding depolarizations.

Arrows indicate time points at which flashes were applied.

dual 10 ms depolarizations did not prevent the C_m response to a subsequent flash (Figure 3C), and analysis of the exocytic burst still revealed two kinetic components, with, for this example, time constants of 31 and 332 ms (Figure 3C, inset).

Figure 4A summarizes the results from experiments in which flashes were preceded by either no depolarizations (Figure 4Aa), the dual 10 ms depolarization protocol (Figure 4Ab), the dual 100 ms depolarization protocol (Figure 4Ac), or the quadruple 100 ms depolarization protocol (four 100 ms depolarizations at 100 ms intervals; Figure 4Ad). From the overlay of the first second of the flash responses (Figure 4B), it becomes clear that the stronger the preflash stimulus, the smaller the amplitude of the exocytic burst. The reduction of the amplitude of the burst could be completely attributed to a decrease in the amplitude of the fast kinetic component, which was virtually absent after the quadruple 100 ms depolarization protocol. Importantly, neither the two time constants, nor the amplitude of the slower kinetic component, were affected by the preceding depolarizations (Figure 4C). Three important conclusions can be drawn from these results. First, depletion of the RRP by depolarizations selectively abolishes the fast kinetic component of the exocytic burst. Note that the amplitude of the fast component (180 fF, corresponding to ~140 vesicles) lies well between the lower (S) and upper (B_{max}) pool size estimate for the RRP obtained with the dual 100 ms protocol (136–205 fF; Figure 2E). Second, the IRP (38–49 fF; Figure 2D) does not show up as a separate kinetic component in the burst but constitutes only ~25% of the fast kinetic component. Therefore, the IRP seems not to be a separate pool of vesicles with fast fusion kinetics but rather a subpool of the RRP experiencing higher Ca^{2+} levels during depolarizations. Third, the slow kinetic component of the exocytic burst corresponds to vesicles that apparently do not fuse upon depolarization.

Recovery of the Exocytic Burst

As flash photolysis of caged Ca^{2+} elevates $[Ca^{2+}]_i$ in a spatially uniform manner, the slow kinetic component of the exocytic burst is not likely to originate from vesicles that experience lower Ca^{2+} concentrations but rather from vesicles undergoing exocytosis at an intrinsically slower rate. Such a slower rate could, for example, reflect that these vesicles have to undergo a last maturation and/or mobilization step before reaching maximal fusion competence. Alternatively, the slower kinetic component may represent the intrinsically slower fusion of an independent population of vesicles. Evidence in favor of the former model was obtained from experiments designed to measure recovery of the RRP. In these experiments, we depleted the RRP by applying the quadruple 100 ms depolarization protocol, as in Figure 4Ad, and then examined refilling by applying flashes after variable intervals (Figure 5A). An overlay of the first second of the flash responses demonstrates that, although the fast kinetic component reappears within 3 s, more than 30 s are required for a complete recovery of the exocytic burst (Figure 5B). A more detailed analysis of the flash responses reveals that the initial rapid recovery of the fast kinetic component of the burst is perfectly mirrored by an equivalent decrease of the slow kinetic component, after which both the fast and the slow component increase in parallel to their respective steady state (Figure 5C). This behavior is exactly what one expects when the slow kinetic component of the burst represents a pool of vesicles in dynamic equilibrium with the RRP (see Discussion).

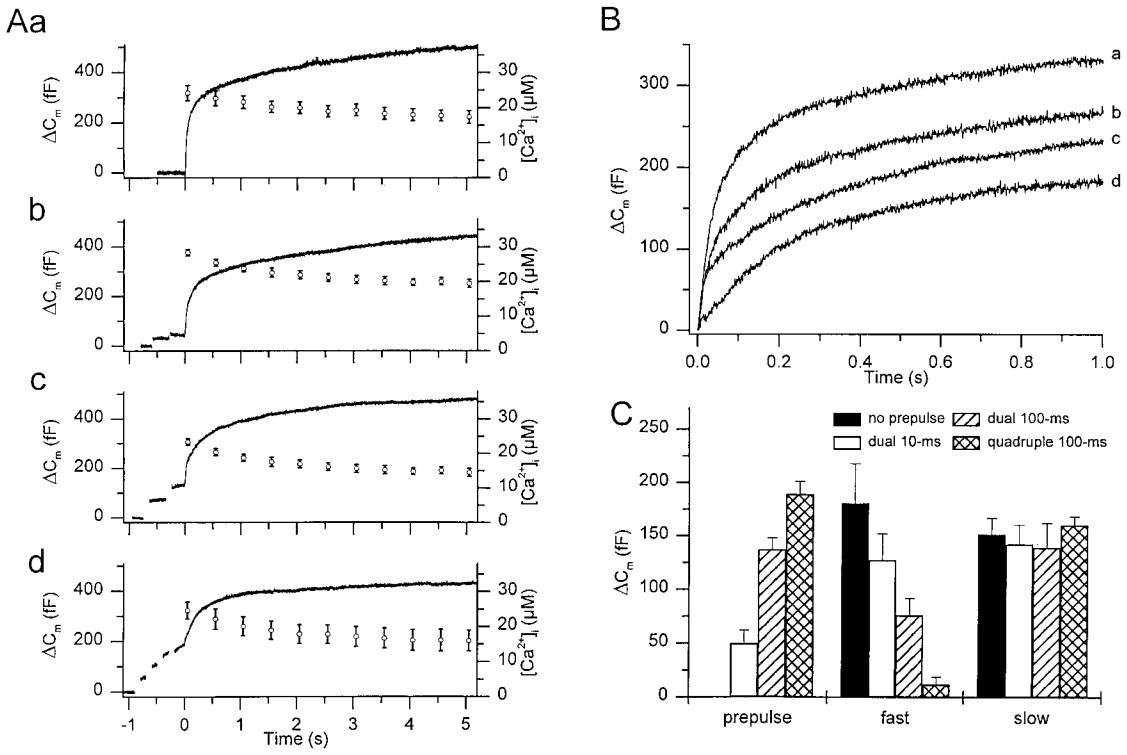

Figure 4. Depolarization-Induced Exocytosis Selectively Alters the Fast Kinetic Component of the Flash Response

(A) Average $[Ca^{2+}]_i$ (measured using Furaptra) and C_m response to a flash preceded by either no depolarizations ([a], n = 18), the dual 10 ms depolarization protocol ([b], n = 16), the dual 100 ms depolarization protocol ([c], n = 19), or the quadruple 100 ms depolarization protocol ([d], n = 14). In these traces, time 0 corresponds to the time of the flash.

(B) Overlay of the first second after the flash of the C_m traces from (A).

(C) Average amplitudes of the C_m response to the prepulse and of the fast and slow kinetic component of the burst for the different protocols shown in (A). The C_m response to the prepulse was estimated from the last 100 ms of the C_m trace before the flash. The kinetic components of the burst were quantified by fitting the sum of three exponential terms to the full 10 s of the flash response. Values for the fast time constant (26 ± 5, 27 ± 7, 22 ± 6, and 25 ± 4 ms, respectively) and for the slow time constant (376 ± 46, 328 ± 85, 401 ± 51, and 338 ± 53 ms, respectively) were not significantly different between the different protocols.

Discussion

The presence of both a fast phasic and a slow, more sustained release component has been demonstrated in a large number of neuronal and neuroendocrine preparations (Rahamimoff and Yaari, 1973; Goda and Stevens, 1994; Horrigan and Bookman, 1994; Hsu and Jackson, 1996; Mennerick and Matthews, 1996; Seward and Nowycky, 1996; Moser and Neher, 1997b; Sakaba et al., 1997; von Gersdorff et al., 1998; Yawo, 1999). Three fundamentally different mechanisms have been discussed to explain this biphasic secretory behavior. First, the fast and slow phase could represent exocytosis of an immediately releasable pool of vesicles and mobilization of vesicles from a reserve pool to the releasable pool, respectively. Second, the fast and slow phase could originate from two pools of equally fusion-competent vesicles that experience different $[Ca^{2+}]_i$ levels due to their localization with respect to Ca^{2+} channels. Finally, the two components could originate from distinct vesicle types, (e.g., large dense-core vesicles versus small synaptic-like vesicles; see Ninomiya et al., 1997; Kasai, 1999) or vesicles with distinct Ca^{2+}-sensing machinery (Geppert et al., 1994; Goda and Stevens, 1994; Yawo, 1999), undergoing exocytosis at intrinsically different rates.

The present study was designed to investigate which of the above mechanisms applies to the biphasic secretory behavior of mouse chromaffin cells in situ. By combining depolarizations with flash photolysis of caged Ca^{2+}, we show that a readily releasable pool of ~140 equally fusion-competent vesicles mediates both the fast phasic and the slower sustained component of depolarization-induced secretion. Vesicles in the RRP fuse at a rate of ~30 s^{-1} when $[Ca^{2+}]_i$ is rapidly and uniformly raised to ~20 μM, which corresponds to the fast kinetic component of the exocytic burst. The fast phasic release is mediated by an IRP of ~35 vesicles, which are rapidly (~150 s^{-1}) released in response to short depolarizations. Three lines of evidence indicate that the IRP constitutes a subpool of the RRP. First, the IRP and RRP are equally sensitive to PMA treatment, which causes a ~50% increase in the size of both pools. Second, recovery of the RRP (Figure 5C) and IRP (Moser and Neher, 1997b) occurs at a comparable rate. Third, the IRP has no specific counterpart in the flash response but just constitutes ~25% of the fast kinetic component of the exocytic burst. We therefore conclude that the IRP corresponds

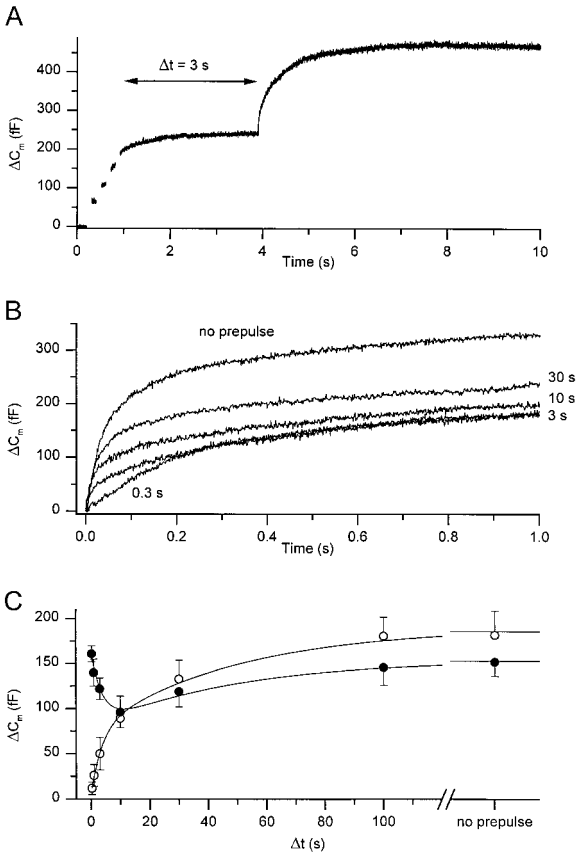

Figure 5. Recovery of the RRP

(A) Illustration of the protocol for measuring the recovery of the RRP. A flash was applied at various intervals after the quadruple 100 ms protocol.

(B) Overlay of the first second of average C_m responses to flashes applied at the indicated intervals after the quadruple 100 ms protocol.

(C) Amplitude of the fast (open circles) and slow (closed circles) component of the exocytic burst at different intervals after the quadruple 100 ms protocol. Each data point represents pooled data from 13–21 cells. The solid lines represent the best fit obtained with the model shown in Figure 6.

to those release-ready vesicles that experience significantly higher Ca^{2+} concentrations during depolarizations, most likely due to a close colocalization with Ca^{2+} channels. If we assume a third power relation between fusion rate and $[Ca^{2+}]_i$ (Heinemann et al., 1993), it follows that vesicles in the IRP experience a Ca^{2+} concentration of ~35 μM during depolarizations. Such high Ca^{2+} levels are only likely to be reached in a microdomain of 10–20 nm from the mouth of a Ca^{2+} channel (Neher, 1998) or within a cluster of several Ca^{2+} channels (Roberts, 1994; Robinson et al., 1995). Longer or repeated depolarizations evoke the slower, more sustained release of the remaining ~105 vesicles in the RRP. The observed fusion rate of ~5 s^{-1} is consistent with vesicles that experience Ca^{2+} concentrations in the range of 5–10 μM, which is likely to occur in the entire submembrane region during prolonged Ca^{2+} influx (Nowycky and Pinter, 1993; Chow et al., 1994; Klingauf and Neher, 1997).

A Refined Model for Secretion in Chromaffin Cells

In previous studies, the amplitude of the exocytic burst after flash photolysis of caged Ca^{2+} was often interpreted as the total number of release-ready vesicles, corresponding to the RRP as defined by depolarizations (Gillis et al., 1996; Xu et al., 1998). However, our present data indicate that the RRP does not correspond to the full exocytic burst but only to the fast kinetic component thereof. The question then arises of what the slower kinetic component of the exocytic burst represents. Two of our findings indicate that this slower kinetic component corresponds to an intermediate pool of ~130 vesicles in dynamic equilibrium with the RRP. First, the initial recovery of the RRP is mirrored by an equivalent decrease in the amplitude of the slow kinetic component of the burst, indicating the transition of less fusion-competent vesicles to the RRP. Second, recovery of the RRP was much slower after a flash than after depolarizations. Indeed, responses to depolarizations were completely suppressed for at least 4 s after a flash (Figure 3B), whereas the RRP recovered >30% in the same time span after the quadruple 100 ms depolarization protocol (Figure 5C). This indicates that the flash also depletes the pool of vesicles that serves to replenish the RRP. These considerations are included in a refined model for secretion from chromaffin cells (Figure 6). In this model, a chromaffin vesicle can occur in three different states. The RRP contains 140 fully fusion-competent chromaffin vesicles that only require a rise in $[Ca^{2+}]_i$ for exocytosis. These vesicles fuse at a rate of 30 s^{-1} when $[Ca^{2+}]_i$ is uniformly raised to 20 μM, which we observe as the rapid component of the exocytic burst. The IRP is a subpool of the RRP, containing 35 vesicles with the same fusion competence but located in the close vicinity of Ca^{2+} channels. This close colocalization enables these vesicles to be rapidly (150 s^{-1}) and selectively released in response to short depolarizations. The slowly releasable pool (SRP) is a pool of 130 vesicles that have to undergo only one rapid maturation/mobilization step before reaching maximal fusion competence. The slower fusion (3 s^{-1}) of the vesicles in the SRP makes up the slow kinetic component of the exocytic burst. Vesicle supply to the SRP is assumed to occur at a slow rate but from a depot pool of 4000 vesicles (Heinemann et al., 1993).

The transition of vesicles between the three different states can be described in matrix notation by

$$\frac{dP}{dt} = \begin{pmatrix} -k_1 & k_{-1} & 0 \\ k_1 & -(k_{-1}+k_2) & k_{-2} \\ 0 & k_2 & -k_{-2} \end{pmatrix} \cdot P \qquad (2)$$

where k_1, k_{-1}, k_2, and k_{-2} are the rate constants and P, which equals (depot SRP RRP)^T, is the vector of the sizes of the respective pools. Equation 2 was numerically solved using a fourth-order Runge-Kutta integration scheme, and a simplex method was used to find the values for the rate constants that gave the best fit to the experimental results in Figure 5C. The resulting values are given in Figure 6. Note that these rate constants and pool sizes may only be valid at the basal $[Ca^{2+}]_i$ in our experiments (~250 nM), as also transitions before the final fusion step are known to be Ca^{2+} dependent (von Ruden and Neher, 1993; Smith et al., 1998).

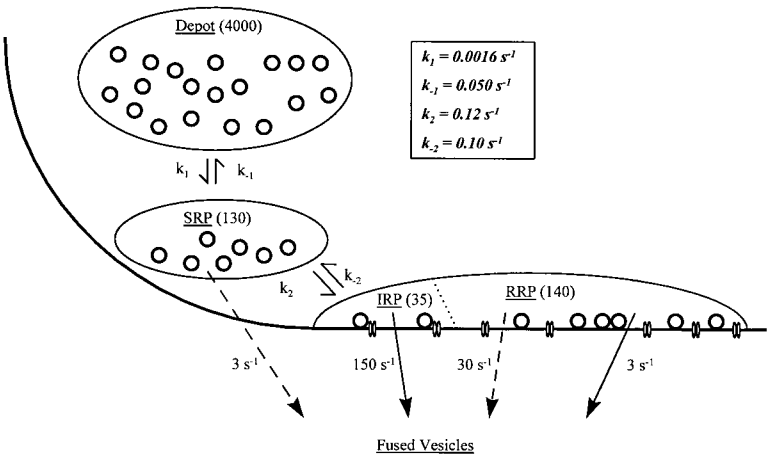

Figure 6. Model

We consider three different vesicle pools, representing three different vesicle maturation states. Note that our scheme does not necessarily imply that vesicles in the SRP and the depot pool reside further away from the plasma membrane than vesicles in the RRP. The estimated number of vesicles in each pool at steady state is indicated in brackets. Rate constants for the transitions between the distinct pools were obtained by fitting the model to the data of Figure 5C. The IRP is a subpool of the RRP, more closely colocalized with Ca^{2+} channels. The fusion rates come from depolarization experiments (solid arrows) or flash experiments ($[Ca^{2+}]_i \approx 20\ \mu M$, broken arrows). See text for more details.

Moreover, the rate constants may well be temperature dependent, such that transitions between pools become faster at physiological temperature.

The transition rate from the SRP to the RRP under the conditions of Figure 5C ($0.12\ s^{-1}$) is too slow to account for the second kinetic component of the exocytic burst, which has a time constant of ~350 ms at ~20 μM (see also Heinemann et al., 1994). We considered two distinct mechanisms to explain this slow kinetic component of the exocytic burst. The transition from the SRP to the RRP may be Ca^{2+} dependent, such that k_2 increases from 0.12 to $\sim 3\ s^{-1}$ after a step increase of $[Ca^{2+}]_i$ to ~20 μM. Alternatively, vesicles from the SRP pool may be able to fuse directly with the plasma membrane at sufficiently high $[Ca^{2+}]_i$, without passing through the RRP. Although our data do not allow choosing between both possibilities, some experimental findings seem to favor the latter mechanism. First, ~5% of the cells in this study did not show a C_m response to depolarizations and did not display a fast kinetic component in the exocytic burst. However, the time course and amplitude of the slow kinetic component of the burst in these cells were not different from cells that displayed a clear fast component. Second, treatment of isolated chromaffin cells with botulinum neurotoxin A was found to fully eliminate the fast kinetic component of the burst, without affecting the slower component (Xu et al., 1998). These observations indicate that, although the transition of vesicles between SRP and RRP seems to be impaired in these cells, secretion from the SRP at high $[Ca^{2+}]_i$ is not affected. Therefore, our model allows for the direct fusion of vesicles from the SRP, albeit with a 10 times slower rate than fusion from the RRP.

Note that the RRP, SRP, and depot pool should not be strictly viewed as vesicle populations residing at increasing distances from the plasma membrane. Recent morphological studies have shown that the number of chromaffin vesicles closely approaching the plasma membrane (morphologically docked vesicles) exceeds the number of release-ready vesicles as determined in electrophysiological experiments by a factor of 2–8 (Parsons et al., 1995; Plattner et al., 1997; Steyer et al., 1997). We therefore prefer to consider the three pools as specific functional states characterized by the maturation stage of the fusion machinery. The refined model presented in this work may facilitate the important task of correlating these functional vesicle pools with specific biochemically defined macromolecular complexes of synaptic proteins (Südhof, 1995; Ryan, 1998; Sutton et al., 1998; Fiebig et al., 1999; Hilfiker et al., 1999).

Exocytic Burst versus Releasable Pools

It is generally accepted that secretion from neurons and neuroendocrine cells initially proceeds from a limited pool of fusion-competent vesicles, but much less consensus exists regarding the size of this RRP. In chromaffin cells, for example, reported RRP size estimates range from 15 to 800 vesicles, depending on the methods used (capacitance measurement, morphometry, evanescent wave microscopy) and/or the stimulation protocol (short or long depolarizations, photorelease of caged Ca^{2+}) (von Ruden and Neher, 1993; Horrigan and Bookman, 1994; Vitale et al., 1995; Gillis et al., 1996; Xu et al., 1998; Oheim et al., 1999). Our present results may help to reconcile some of the contradictory results in the literature. First, the exocytic burst after photorelease of caged calcium has been used as an estimate of the RRP. According to our present findings, however, this results in an overestimate, as the exocytic burst consists of both the RRP and the SRP. Second, depending on the amount of voltage-dependent Ca^{2+} influx, pool size estimates from dual-pulse protocols may reflect either the whole RRP or only the IRP. Third, capacitance responses to trains of depolarizations may overestimate the RRP, since significant refilling of the RRP from the SRP can be expected during these relatively extended protocols. Fourth, the size of the RRP changes dramatically with basal $[Ca^{2+}]_i$ (von Ruden and Neher, 1993; Smith et al., 1998). In our flash experiments, basal $[Ca^{2+}]_i$ was buffered to the relatively high value of 250 nM, due to the requirement of a sufficient Ca^{2+} loading of NP-EGTA. Differences in basal $[Ca^{2+}]_i$ under different recording situations may lead to widely discrepant pool size estimates.

Rapid Exocytosis from Neuroendocrine Cells: A Waste of Timing?

Our results indicate that chromaffin cells in situ contain an IRP of release-ready vesicles in the close vicinity of

Ca^{2+} channels, which can be released by short depolarizations at a remarkably high rate of 150 s^{-1}, comparable to release rates observed in neuronal preparations (Goda and Stevens, 1994; Hsu and Jackson, 1996; Mennerick and Matthews, 1996; Yawo, 1999). Whereas a tight stimulus–secretion coupling in presynaptic nerve terminals is a prerequisite for rapid synaptic transmission, it may at first sight seem useless in neuroendocrine cells. Indeed, as the secreted hormones exert their action mainly at distant cells and organs, the rate-limiting step is no longer the fusion but rather the time required for the hormone to be transported to the target organs through the bloodstream. However, our present results may point at another physiological role for a tight stimulus–secretion coupling in neuroendocrine cells. We show that the IRP can be rapidly and selectively released by moderate stimuli, without noticeable global rise in $[Ca^{2+}]_i$. Chromaffin cells may exploit this tight stimulus–secretion coupling to provide a basal catecholamine level at minimal metabolic expenditure. Only at sufficiently high stimulus intensity, $[Ca^{2+}]_i$ will rise globally and trigger the additional fusion of release-ready vesicles more distal to Ca^{2+} channels. In conjunction with the rapid supply of vesicles from the SRP, this may underlie the massive burst of catecholamine release that occurs in periods of stress.

Experimental Procedures

Adrenal Slice Preparation and Whole-Cell Recordings

Adrenal glands from 4- to 10-week-old NMRI mice were used. Slices (120–170 μm thick) were prepared as previously described (Moser and Neher, 1997b). Slices were used starting shortly after cutting for 6–8 hr.

Whole-Cell Capacitance Measurements

For recording, slices were fixed in the recording chamber by means of a grid of nylon threads. After mounting onto the stage of an upright microscope (Axioscope, Zeiss), the chamber was perfused at a flow rate of 1–2 ml/min with BBS, which contained (in mM) 125 NaCl, 26 $NaHCO_3$, 2.5 KCl, 1.25 NaH_2PO_4, 2 $CaCl_2$, 1 $MgCl_2$, 10 glucose, and 0.2 d-tubocurarine, bubbled to pH 7.4 with 95% O_2 and 5% CO_2. Usually a cleaning pipette was used to remove loose material from the cell surface. Conventional whole-cell recordings (Hamill et al., 1981) were performed with 3–4 MΩ pipettes, and an EPC-9 patch-clamp amplifier together with Pulse software (HEKA, Lambrecht, Germany) was used. Pipette solution 1, which was used for the normal depolarization experiments, contained (in mM) 145 Cs-glutamate, 8 NaCl, 1 $MgCl_2$, 2 Mg-ATP, 0.3 Na_2-GTP, 10 Cs-HEPES, and 0.1 Fura-2. For flash experiments, pipette solution 2 was used, which contained (in mM) 125 Cs-glutamate, 8 NaCl, 1 $MgCl_2$, 2 Mg-ATP, 0.3 Na_2-GTP, 10 Cs-HEPES, 5 nitrophenyl-EGTA, 3.75 $CaCl_2$, and 0.5 Furaptra. The concentration of free Ca^{2+} in the latter solution was measured to be ~250 nM. Pipette solutions were titrated to pH 7.2 and their osmolality was 300 mOsm. The liquid junction potentials of the extracellular solution against the Cs-glutamate-based internal solutions were measured to be +10 mV, and all clamp potentials were corrected accordingly. Experiments were carried out at room temperature.

Capacitance measurements were performed using the Lindau-Neher technique implemented as the "sine + dc" mode of the "software lock-in" extension of PULSE software. A 1 kHz, 70 mV peak-to-peak sinusoid stimulus was applied about a DC holding potential of −80 mV. Data were acquired through a combination of the high time resolution PULSE software and the lower time resolution X-Chart plug-in module to the PULSE software.

Two methods were used to eliminate influences of nonsecretory capacitance transients after depolarizations (Horrigan and Bookman, 1994; Moser and Neher, 1997b): (1) when possible, C_m was analyzed in a window between 1 and 2.5 s after the depolarization, or alternatively (2) the nonsecretory C_m responses were measured late in the experiments after exhaustion of secretion, and exponential fits to these late responses were subtracted from early C_m responses. To estimate the number of fused vesicles from C_m changes, we used the estimation of a mean capacitance of 1.3 fF per vesicle (Moser and Neher, 1997a).

Measurements of $[Ca^{2+}]_i$ and Photolysis of Caged Ca^{2+}

$[Ca^{2+}]_i$ was measured by dual-wavelength ratiometric fluorimetry with the indicator dyes Fura-2 or Furaptra. The dyes were excited with light alternated between 360 and 390 nm using a monochromator-based system (TILL photonics, Planegg, Germany), and the resulting fluorescent signal was measured using a photomultiplier. $[Ca^{2+}]_i$ was determined from ratio R of the fluorescent signals at both wavelengths following:

$$[Ca^{2+}]_i = K_{eff} (R - R_{min})/(R_{max} - R) \quad (3)$$

where K_{eff}, R_{min}, and R_{max} are calibration constants obtained from in vivo calibrations. To obtain step-wise increases in $[Ca^{2+}]_i$, 75% calcium-saturated NP-EGTA was loaded into the cell (pipette solution 2), and flashes of ultraviolet light were applied to the whole cell. As the flash photolysis efficiency of a 375 V discharge flash was measured to be 45%, we used neutral-density filters transmitting 50%–65% of the flash light resulting in $[Ca^{2+}]_i$ values of ~20 μM. To keep a relatively stable $[Ca^{2+}]_i$ level following a flash, the monochromator light was used both to measure $[Ca^{2+}]_i$ and to release additional caged Ca^{2+} (Xu et al., 1998). Calibration constants for Furaptra were determined both before and after a full flash, to compensate for the effects of bleaching of Furaptra and NP-EGTA on the measured postflash fluorescence ratio.

Acknowledgments

We would like to thank Drs. Jürgen Klingauf and Corey Smith for critical comments on the manuscript and Dr. Tao Xu for help setting up the caged Ca^{2+} experiments. T. V. is a postdoctoral researcher of the Flemish Fund for Scientific Research. This work was supported by a grant from the Deutsche Forschungsgemeinschaft (SFB 523).

Received May 3, 1999; revised June 2, 1999.

References

Chow, R.H., Klingauf, J., and Neher, E. (1994). Time course of Ca^{2+} concentration triggering exocytosis in neuroendocrine cells. Proc. Natl. Acad. Sci. USA *91*, 12765–12769.

Dodge, F.A., Jr., and Rahamimoff, R. (1967). Co-operative action of calcium ions in transmitter release at the neuromuscular junction. J. Physiol. *193*, 419–432.

Fiebig, K.M., Rice, L.M., Pollock, E., and Brunger, A.T. (1999). Folding intermediates of SNARE complex assembly. Nat. Struct. Biol. *6*, 117–123.

Geppert, M., Goda, Y., Hammer, R.E., Li, C., Rosahl, T.W., Stevens, C.F., and Südhof, T.C. (1994). Synaptotagmin I: a major Ca^{2+} sensor for transmitter release at a central synapse. Cell *79*, 717–727.

Gillis, K.D., Mossner, R., and Neher, E. (1996). Protein kinase C enhances exocytosis from chromaffin cells by increasing the size of the readily releasable pool of secretory granules. Neuron *16*, 1209–1220.

Goda, Y., and Stevens, C.F. (1994). Two components of transmitter release at a central synapse. Proc. Natl. Acad. Sci. USA *91*, 12942–12946.

Grynkiewicz, G., Poenie, M., and Tsien, R.Y. (1985). A new generation of Ca^{2+} indicators with greatly improved fluorescence properties. J. Biol. Chem. *260*, 3440–3450.

Hamill, O.P., Marty, A., Neher, E., Sakmann, B., and Sigworth, F.J. (1981). Improved patch-clamp techniques for high-resolution current recording from cells and cell-free membrane patches. Pflügers Arch. *391*, 85–100.

Heidelberger, R., Heinemann, C., Neher, E., and Matthews, G. (1994).

Calcium dependence of the rate of exocytosis in a synaptic terminal. Nature *371*, 513–515.

Heinemann, C., von Ruden, L., Chow, R.H., and Neher, E. (1993). A two-step model of secretion control in neuroendocrine cells. Pflügers Arch. *424*, 105–112.

Heinemann, C., Chow, R.H., Neher, E., and Zucker, R.S. (1994). Kinetics of the secretory response in bovine chromaffin cells following flash photolysis of caged Ca^{2+}. Biophys. J. *67*, 2546–2557.

Hilfiker, S., Greengard, P., and Augustine, G.J. (1999). Coupling calcium to SNARE-mediated synaptic vesicle fusion. Nat. Neurosci. *2*, 104–106.

Horrigan, F.T., and Bookman, R.J. (1994). Releasable pools and the kinetics of exocytosis in adrenal chromaffin cells. Neuron *13*, 1119–1129.

Hsu, S.F., and Jackson, M.B. (1996). Rapid exocytosis and endocytosis in nerve terminals of the rat posterior pituitary. J. Physiol. *494*, 539–553.

Kasai, H. (1999). Comparative biology of Ca^{2+}-dependent exocytosis: implications of kinetic diversity for secretory function. Trends Neurosci. *22*, 88–93.

Klingauf, J., and Neher, E. (1997). Modeling buffered Ca^{2+} diffusion near the membrane: implications for secretion in neuroendocrine cells. Biophys. J. *72*, 674–690.

Mennerick, S., and Matthews, G. (1996). Ultrafast exocytosis elicited by calcium current in synaptic terminals of retinal bipolar neurons. Neuron *17*, 1241–1249.

Minami, N., Berglund, K., Sakaba, T., Kohmoto, H., and Tachibana, M. (1998). Potentiation of transmitter release by protein kinase C in goldfish retinal bipolar cells. J. Physiol. *512*, 219–225.

Moser, T., and Neher, E. (1997a). Estimation of mean exocytic vesicle capacitance in mouse adrenal chromaffin cells. Proc. Natl. Acad. Sci. USA *94*, 6735–6740.

Moser, T., and Neher, E. (1997b). Rapid exocytosis in single chromaffin cells recorded from mouse adrenal slices. J. Neurosci. *17*, 2314–2323.

Neher, E. (1998). Vesicle pools and Ca^{2+} microdomains: new tools for understanding their roles in neurotransmitter release. Neuron *20*, 389–399.

Neher, E., and Marty, A. (1982). Discrete changes of cell membrane capacitance observed under conditions of enhanced secretion in bovine adrenal chromaffin cells. Proc. Natl. Acad. Sci. USA *79*, 6712–6716.

Ninomiya, Y., Kishimoto, T., Yamazawa, T., Ikeda, H., Miyashita, Y., and Kasai, H. (1997). Kinetic diversity in the fusion of exocytotic vesicles. EMBO J. *16*, 929–934.

Nowycky, M.C., and Pinter, M.J. (1993). Time courses of calcium and calcium-bound buffers following calcium influx in a model cell. Biophys. J. *64*, 77–91.

Oheim, M., Loerke, D., Stuhmer, W., and Chow, R.H. (1999). Multiple stimulation-dependent processes regulate the size of the releasable pool of vesicles. Eur. Biophys. J. *28*, 91–101.

Parsons, T.D., Coorssen, J.R., Horstmann, H., and Almers, W. (1995). Docked granules, the exocytic burst, and the need for ATP hydrolysis in endocrine cells. Neuron *15*, 1085–1096.

Plattner, H., Artalejo, A.R., and Neher, E. (1997). Ultrastructural organization of bovine chromaffin cell cortex—analysis by cryofixation and morphometry of aspects pertinent to exocytosis. J. Cell Biol. *139*, 1709–1717.

Rahamimoff, R., and Yaari, Y. (1973). Delayed release of transmitter at the frog neuromuscular junction. J. Physiol. *228*, 241–257.

Roberts, W.M. (1994). Localization of calcium signals by a mobile calcium buffer in frog saccular hair cells. J. Neurosci. *14*, 3246–3262.

Robinson, I.M., Finnegan, J.M., Monck, J.R., Wightman, R.M., and Fernandez, J.M. (1995). Colocalization of calcium entry and exocytotic release sites in adrenal chromaffin cells. Proc. Natl. Acad. Sci. USA *92*, 2474–2478.

Ryan, T.A. (1998). Probing a complex question: when are SNARE proteins ensnared? Nat. Neurosci. *1*, 175–176.

Sakaba, T., Tachibana, M., Matsui, K., and Minami, N. (1997). Two components of transmitter release in retinal bipolar cells: exocytosis and mobilization of synaptic vesicles. Neurosci. Res. *27*, 357–370.

Seward, E.P., and Nowycky, M.C. (1996). Kinetics of stimulus-coupled secretion in dialyzed bovine chromaffin cells in response to trains of depolarizing pulses. J. Neurosci. *16*, 553–562.

Smith, C., Moser, T., Xu, T., and Neher, E. (1998). Cytosolic Ca^{2+} acts by two separate pathways to modulate the supply of release-competent vesicles in chromaffin cells. Neuron *20*, 1243–1253.

Stevens, C.F., and Sullivan, J.M. (1998). Regulation of the readily releasable vesicle pool by protein kinase C. Neuron *21*, 885–893.

Steyer, J.A., Horstmann, H., and Almers, W. (1997). Transport, docking and exocytosis of single secretory granules in live chromaffin cells. Nature *388*, 474–478.

Südhof, T.C. (1995). The synaptic vesicle cycle: a cascade of protein–protein interactions. Nature *375*, 645–653.

Sutton, R.B., Fasshauer, D., Jahn, R., and Brunger, A.T. (1998). Crystal structure of a SNARE complex involved in synaptic exocytosis at 2.4 Å resolution. Nature *395*, 347–353.

Thomas, P., Wong, J.G., Lee, A.K., and Almers, W. (1993). A low affinity Ca^{2+} receptor controls the final steps in peptide secretion from pituitary melanotrophs. Neuron *11*, 93–104.

Vitale, M.L., Seward, E.P., and Trifaro, J.M. (1995). Chromaffin cell cortical actin network dynamics control the size of the release-ready vesicle pool and the initial rate of exocytosis. Neuron *14*, 353–363.

von Gersdorff, H., Sakaba, T., Berglund, K., and Tachibana, M. (1998). Submillisecond kinetics of glutamate release from a sensory synapse. Neuron *21*, 1177–1188.

von Ruden, L., and Neher, E. (1993). A Ca-dependent early step in the release of catecholamines from adrenal chromaffin cells. Science *262*, 1061–1065.

Xu, T., Binz, T., Niemann, H., and Neher, E. (1998). Multiple kinetic components of exocytosis distinguished by neurotoxin sensitivity. Nat. Neurosci. *1*, 192–200.

Yawo, H. (1999). Two components of transmitter release from the chick ciliary presynaptic terminal and their regulation by protein kinase C. J. Physiol. *516*, 461–470.